DOI 10.1007/s11041-023-00942-x
Metal Science and Heat Treatment, Vol. 65, Nos. 5 – 6, September, 2023 (Russian Original Nos. 5 – 6, May – June, 2023)

ADDITIVE TECHNOLOGIES, POWDER AND COMPOSITE MATERIALS

UDC 669.71:663.3:621.762:537.31

INCREASING THE CONDUCTIVITY OF SINTERED POWDER Al – Cu MATERIAL DUE TO ELECTROPLATING OF ALUMINIUM PARTICLES WITH COPPER

N. G. Puteri,[1] Y. W. Yu,[1] and W. H. Lee[1]

Translated from *Metallovedenie i Termicheskaya Obrabotka Metallov*, No. 6, pp. 65 – 72, June, 2023.

Original article submitted October 6, 2022.

An economical Al – Cu powder with high conductivity has been synthesized by a chemical substitution reaction. The powder particles have the form of an aluminium core, on which a copper shell is deposited. The deposition reaction occurs in a copper sulphate solution at a temperature of 45°C. At higher temperatures, copper diffusion proceeds faster, but the aluminium core may crack. The process of aluminium substitution with copper on the particle surface develops at different values of the standard potential of each metal. The minimum resistivity of $1.01 \times 10^{-7}\ \Omega \cdot$ m is obtained in a composite sintered at 550°C from the Al-core Cu-shell powder with addition of 3 wt.% glass frit. This material can find wide application, for example, as a substitute for silver in electronic devices to reduce production costs.

Key words: aluminium, copper, powder material, microstructure, conductivity, electroplating.

INTRODUCTION

Almost all modern fields of technology require the use of materials with high electrical conductivity. The most common among them are metals and alloys. Gold, silver, indium, and lead have the best electrical properties, but they are expensive [1]. Nickel, copper and aluminium are much cheaper, but their conductivity and corrosion resistance are lower. Extremely promising is the creation of materials that combine different metals and combine high conductivity with low cost.

To create such materials, it is of interest to use aluminium as the main precursor. Aluminium is the third most common element in the earth's crust [2] and has a face-centred cubic crystal lattice [3]. The oxidized form of aluminium, i.e. aluminium oxide (Al_2O_3), has mixed ion-covalent bonds, which provides it with high hardness, elastic modulus, wear and corrosion resistance. However, the Al_2O_3 oxide layer limits the contact between the particles, which reduces the conductivity of the powder material. To increase its conductivity, it is advisable to create materials with a complex structure, i.e. with a core-shell structure, consisting of a solid core coated with one or several different materials with high conductivity.

Such materials can be synthesized by the liquid-phase method: chemical deposition of a shell element onto a core particle followed by "assembly" of the formed nanoparticles due to electrostatic interaction [4]. This method is based on the Stöber process. It forms an amorphous or crystalline layer from the corresponding salt on the core surface. The reaction leads to homogeneous nucleation and formation of particles in the surrounding liquid phase. Another way is a direct reaction by chemical deposition on the core surface [5, 6].

Chemical deposition on functionalized core particles is difficult due to the hydrophobic nature of the core surface, its insufficient surface charge, and incompatibility with shell

[1] Department of Electrical Engineering, National Cheng Kung University, Tainan, Taiwan R.O.C. (e-mail: leewen@mail.ncku.edu.tw).

materials. The Stöber process makes synthesis possible due to three of its features. First, a reaction occurs between the surface hydroxyl groups of the core particle and the $–OCH_3$ or $–OC_2H_5$ anions from the silane coupling agent [R-$(CH_3)_nSi(OMe)_3$] with the replacement of –OH by the $–R$ group, and the surface is being modified. Second, the corresponding functional silane is absorbed on the surface of non-oxide nanoparticles. Then $–R$ and siloxane cover the surface by hydrolysis of –OMe groups and condense with other types of silica. Third, the addition of a functional silane to the particle surface leads to the formation of a silica shell. Successful implementation of such a synthesis of materials requires the use of the right agents [7 – 9].

When pre-formed nanoparticles are assembled by the method of electrostatic interactions, the core – shell structure is formed due to the opposite charges of the core and shell. The process takes place in the liquid phase of uniformly dispersed core particles. The pH value in the reaction plays a major role, since the process depends on the charge of the core and shell. However, it is necessary to prevent agglomeration of the nanoparticle shell. The assembly of nanoparticles on functionalized core particles is also complicated by the fact that nanoparticles tend to separate from the core surface. To overcome this, there are two methods, such as electrostatic interaction and chemical coordination [10].

The substitution reaction used in this study refers to the assembly of nanoparticles by electrostatic interactions. The mechanism of this reaction is based on the interaction of ions of elements or compounds. The reducing or oxidizing substance is replaced by a relatively weak substance. The value of the standard electrode potential is known, it helps to determine the appropriate conditions for the substitution reaction. Determining the standard electrode potential is also a way of assessing the reducing or oxidizing power of an element. At a pressure of 1 atm and a temperature of 25°C, or the so-called standard state, the value of the potential of the standard hydrogen electrode is set to zero. The sign of the standard value of the electrode (denoted as E°, V) above hydrogen is positive (+), and below hydrogen is negative (–) [8]. The standard potential (E°) of a number of elements is presented in Table 1.

The experiment carried out in [11] between a copper sheet and silver nitrate in an aqueous solution is one of the substitution reactions. During this experiment, dendritic silver particles are formed. Copper emits electrons, and a silver ion joins these electrons and forms a silver particle. The direction of the reaction changes, and the total E value becomes –0.340 V. The reaction of this experiment is expressed by the following equations:

$$Cu(s) \rightarrow Cu^{2+} + 2e^{-}; \quad (1)$$

$$Ag^{+} + e^{-} \rightarrow Ag(s); \quad (2)$$

$$Cu + 2Ag^{+} \rightarrow Cu^{2+} + 2Ag. \quad (3)$$

TABLE 1. Standard Potentials of Chemical Elements [8 – 12]

Ionic equation	E°, V
$Li^{+} + e^{-} \rightarrow Li(s)$	–3.0401
$Na^{+} + e^{-} \rightarrow Na(s)$	–2.71
$Al^{3+} + 3e^{-} \rightarrow Al(s)$	–1.662
$Cl_2(g) + 2e^{-} \rightarrow 2Cl^{-}$	+1.36
$Cu^{2+} + 2e^{-} \rightarrow Cu(s)$	–0.34
$Zn^{2+} + 2e^{-} \rightarrow Zn(s)$	–0.7618
$Ag^{+} + e^{-} \rightarrow Ag(s)$	+0.7996

This method of producing complex compounds can facilitate easy synthesis with low sintering temperature and low production costs.

The objective of this research is to study the possibility of creating an electrically conductive powder material by synthesizing core – shell particles using aluminium powder as the particles core and copper as their shell, applied by the chemical coating method according to the substitution reaction principle.

METHODS OF STUDY

A commercial aluminium powder with a particle size of 5 μm manufactured by Force Applied Material Technology Corp. and copper sulphate produced by Sumitomo Metal Mining Co., Ltd. were used for the study. Aluminium powder was added to a solution of 4.52 mol of copper sulphate heated to 45°C. The mixture was stirred until a noticeable colour change appeared. A green powder was produced by filtration and drying from a solution of aluminium powder with a copper shell. Next, the green powder was mixed with 3 – 9 wt.% glass frit with a particle size of 1.3 μm and sintered in a nitrogen atmosphere at 400, 450, 500, or 550°C.

The microstructure of the produced material was studied using a focused ion beam (LMIS, FEI Co.) and a scanning electron microscope (temic EM200S). The electrical resistivity was measured by the four-point probe method. The samples were made from sintered disks 1.5 mm in diameter and 3 mm thick. Using the measured electrical resistivity values, the conductivity was calculated using the equation:

$$\sigma = \frac{t}{\rho w l}. \quad (4)$$

RESULTS AND DISCUSSION

Aluminium powder was poured into a saturated solution of copper sulphate. At that, an efficient reaction of metal ion replacement on the aluminium powder surface took place in the solution. A noticeable colour change at the first stage of synthesis in the solution from light grey to brownish-reddish, as well as an increase in the solution temperature and gas re-

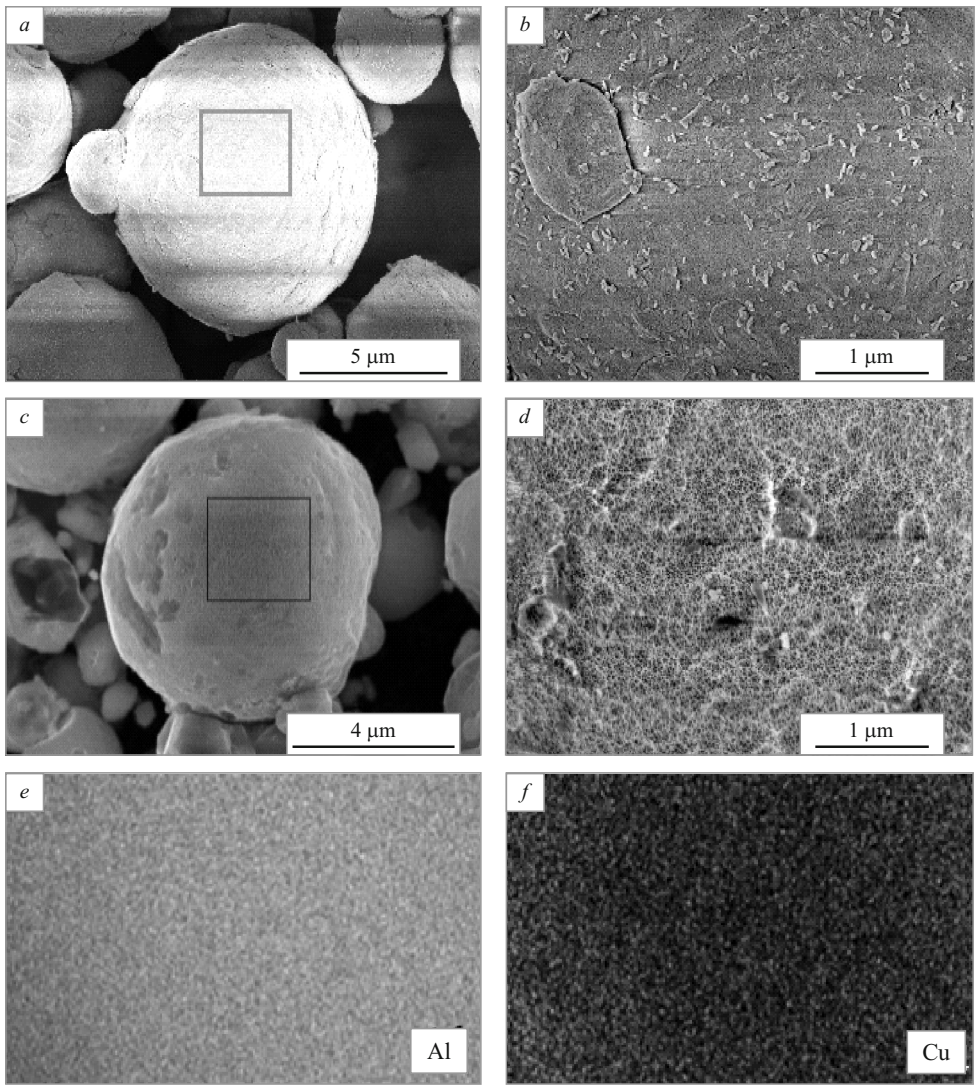

Fig. 1. Structure (SEM) of aluminium powder particles in the initial state (*a*, *b*), after copper coating (*c*, *d*); distribution maps (EDS) of aluminium (*e*) and copper (*f*) in the surface layer of coated particles.

lease, was observed, which was evidence of the reaction. To stabilize the temperature, deionized water was added to the solution. The addition of copper to aluminium was indicated by the appearance of brown-red copper particles on the surface. Taking into account that the result of substitution is affected by the temperature and duration of the reaction, the solution concentration, and the treatment after sintering [12], the most effective values of these parameters were experimentally chosen.

It has been established that the highest density of the copper shell layer on an aluminium core is formed at a copper sulphate solution temperature of 45°C for 40 min. The morphology and composition of the surface of aluminium powder particles before and after copper coating are shown in Fig. 1. The amorphous Cu shell layer can be distinguished by the spongy structure surrounding the Al particles after coating. The presence of Al and Cu elements on the surface of powder particles, respectively, before and after coating deposition was confirmed by energy dispersive spectrometry (Fig. 1*e* and *f*). A study using a focused ion beam shows (Fig. 2) that copper forms a uniform surface layer with an average thickness of 100 nm in a complex Cu – Al core – shell particle.

During the formation of a surface layer on the surface of Al particles in direct contact with a solution of copper sulphate, the following reactions occurred:

$$Al_{(s)} + CuSO_{4(aq)} \rightarrow Cu_{(s)} + Al_2SO_{4(aq)}, \quad (5)$$

$$Al_{(s)} \rightarrow Al^{3-} + 3e^-, \quad (6)$$

$$Cu^{2+} + 2e^- \rightarrow Cu_{(s)}. \quad (7)$$

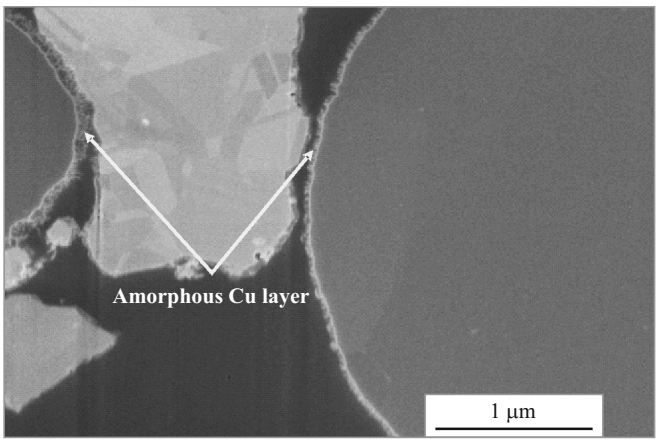

Fig. 2. Structure (FIB image) of Al – Cu core – shell particles.

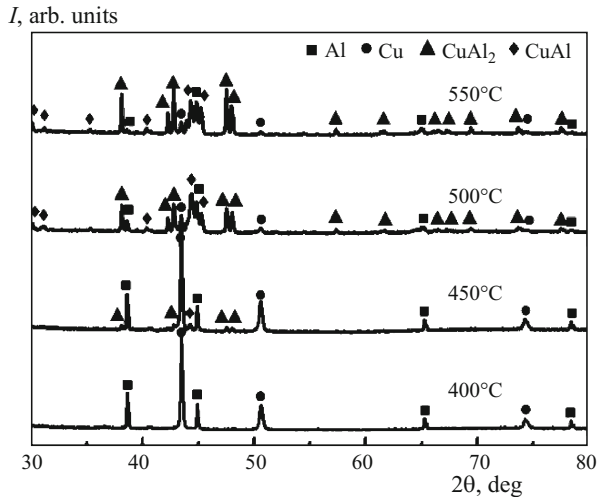

Fig. 3. Diffraction patterns of Al – Cu core – shell particles after sintering at different temperatures (numbers near the curves).

Aluminium ions released into the solution bind with sulphate and form aluminium sulphate. Each Al atom emits three electrons and becomes an Al ion ($Al^o \rightarrow Al^{3-}$) as a result of a spontaneous galvanic reaction controlled by Al^o/Al^{3+} potentials (+1.662 V vs SHE). Meanwhile, the Cu ions in the solution accept electrons and become the Cu metal ($Cu^{2+} \rightarrow Cu^0$) controlled by Cu^{2+}/Cu^0 potential (–0.337 V vs SHE). As a result of these processes, an amorphous Cu layer is formed around the Al particles.

Diffraction patterns of copper-coated volumes of aluminium at different sintering temperatures are shown in Fig. 3. Diffraction peaks of powder particles sintered at 400°C at 33.47°, 44.74°, 65.13°, and 78.23° correspond to (111), (200), (220), and (311) reflections of a cubic aluminium (JCPDS card: 00-004-0787). Peaks at 43.29°, 50.43°, and 74.13° correspond to (111), (200), and (220) reflections of cubic copper (JCPDS card: 00-004-0836). Crystalline phases of copper and aluminium are formed without impurities of other phases. It proves that the powder has been successfully produced, and copper and aluminium have not yet begun to interact.

With an increase in the sintering temperature to 450°C, new peaks appear in the crystalline phases of copper and aluminium at 37.86°, 42.59°, 47.33°, and 47.80°, corresponding to (211), (112), (310) and (202) tetragonal $CuAl_2$ phase (JCPDS card: 00-025-0012). It indicates the occurrence of diffusion processes between the copper shell and the aluminium core, which leads to the formation of an alloy.

After sintering at 500°C, the diffraction patterns show the appearance of additional peaks at 31.06°, 31.55°, 35.09°, 40.17°, 44.18°, and 45.06°, corresponding to (–311), (–402), (–312), (–203), (020), and (–313) reflections of the monoclinic CuAl compound (JCPDS card: 00-026-0016). At that, the intensity of the diffraction peaks of pure metals decreases due to the formation of new $CuAl_2$ and CuAl phases as a result of increased diffusion between copper and aluminium. With an increase in the sintering temperature to 550°C, no noticeable changes in the diffraction patterns compared to 500°C are observed.

Figure 4 shows diffraction patterns from copper-coated aluminium particles with the addition of 3, 6, and 9 wt.% glass frit after sintering at various temperatures. The role of the glass frit is not only to promote sintering by lowering the temperature, but also to act as an insulating layer. Figure 4 shows that the diffraction peaks of the complex Al – Cu core – shell particles with 3 wt.% glass frit are similar to the peaks of the same Al – Cu particles without additives. However, the diffraction peaks of Al – Cu particles with 6 and 9 wt.% glass frits differ from the peaks of Al – Cu particles with 3 wt.% frit but are close to each other. The main difference lies in the fact that the amount of the second $CuAl_2$phase formed at 500°C in the Al – Cu core – shell particles with a lower content of glass frit (0 and 3 wt.%) is significantly higher than that in particles with a larger frit content (6 and 9 wt.%). Obviously, the presence of glass frits between the Al – Cu core – shell particles blocks their contact and prevents the formation of the second $CuAl_2$ phase.

Figure 5 shows the structure and diagrams of the cross-sections of Al – Cu core – shell particles sintered at different temperatures. It has been revealed that the measured porosity is 14.79% after powder sintering at 400°C, 12.35% at 450°C, 4.00% at 500°C, and 2.71% at 550°C. A decrease in the porosity of the material with an increase in the sintering temperature is explained by an increase in the intensity of copper diffusion into aluminium. Moreover, the higher the diffusion, the higher the number of interparticle bonds (Fig. 5).

Thus, the effect of glass frit on the phase composition and porosity of Al – Cu core – shell particles increases with an increase in the temperature of their formation process. It agrees with the Al – Cu phase diagram [13]. According to the diagram, at 4 wt.% Cu binary Al – Cu compound appears only at temperatures above 450°C, at which $\alpha + \theta$ phases are

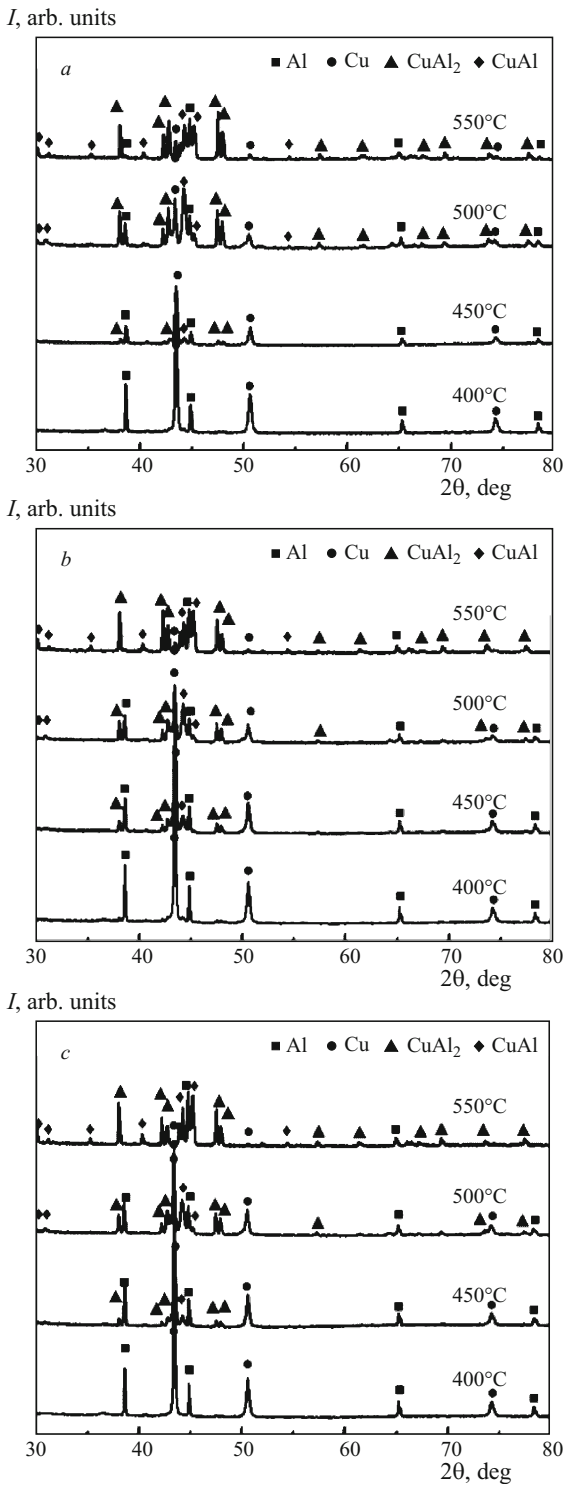

Fig. 4. Diffraction patterns of Al – Cu core – shell particles with a glass frit in the amount of 3 wt.% (*a*), 6 wt.% (*b*), and 9 wt.% (*c*) after sintering at different temperatures (numbers near the curves).

formed. α phase is a solid solution of aluminium and copper, and θ phase is brittle $CuAl_2$ intermetallic [14, 15]. This intermetallic compound, formed between the particles, can block the electric current. It should be noted that the sintering temperature used in this study is limited to 550°C, since it is near the solvus line [16].

TABLE 2. Electrical Resistivity of Al – Cu Powder with Different Contents of Glass Frit

T_{sp}, °C	ρ, Ω · m, with glass frit content, wt.%			
	0	3	6	9
450	3.76×10^{-3}	1.60×10^{-3}	2.18×10^{-3}	4.65×10^{-3}
500	8.33×10^{-6}	3.09×10^{-6}	4.86×10^{-6}	5.83×10^{-6}
550	2.07×10^{-7}	1.01×10^{-7}	1.48×10^{-7}	2.13×10^{-7}
600	8.66×10^{-7}	2.52×10^{-7}	1.19×10^{-6}	3.26×10^{-6}

Notations: T_{sp} is the sintering temperature Al – Cu core – shell powder particles; ρ is the electrical resistivity.

Figure 6 shows the structure of the cross section of Al – Cu core – shell particles with 3, 6, 9 wt.% glass frits sintered at 500 and 550°C. The glass frit can promote contact between the Al – Cu particles as a result of liquid-phase sintering; therefore, with an increase in the glass frit content in the material, the microstructure of the particles becomes denser, and the crystallinity of the Al – Cu grain increases the more, the higher the sintering temperature.

The liquid phase of the glass frit reduces the porosity of the material and increases the bond between the particles. However, according to Table 2, the Al – Cu material with 3 wt.% glass frit, sintered at 550°C, has the lowest electrical resistivity. Probably, a larger amount of glass frit, although it increases the bond between the particles, has an insulating effect on the material, making it difficult for electrons to pass through and, as a result, reducing conductivity. At the same time, the conductivity of Al – Cu particles without a glass frit is lower than that of the core and shell with the addition of a glass frit. Thus, glass frits, improving interparticle bonds, increase the electron transfer current. However, the insulating effect of frits at their high content increases the electrical resistivity of the material, which requires control of the glass frit amount added to the powder.

CONCLUSIONS

1. The possibility of synthesizing the electrically conductive Al – Cu core – shell material by applying copper to the surface of aluminium powder particles by the method of chemical coating according to the substitution reaction principle, as well as the effect on its properties of adding 3 – 9 wt.% glass frit with a particle size of 1.3 μm and of sintering temperature (400 – 550°C) in a nitrogen atmosphere, has been studied.

2. Composite powder particles from a copper layer 100 nm thick on an aluminium particle 2 μm thick were successfully produced using the galvanic substitution reaction of aluminium in a copper sulphate solution at 45°C for 40 min.

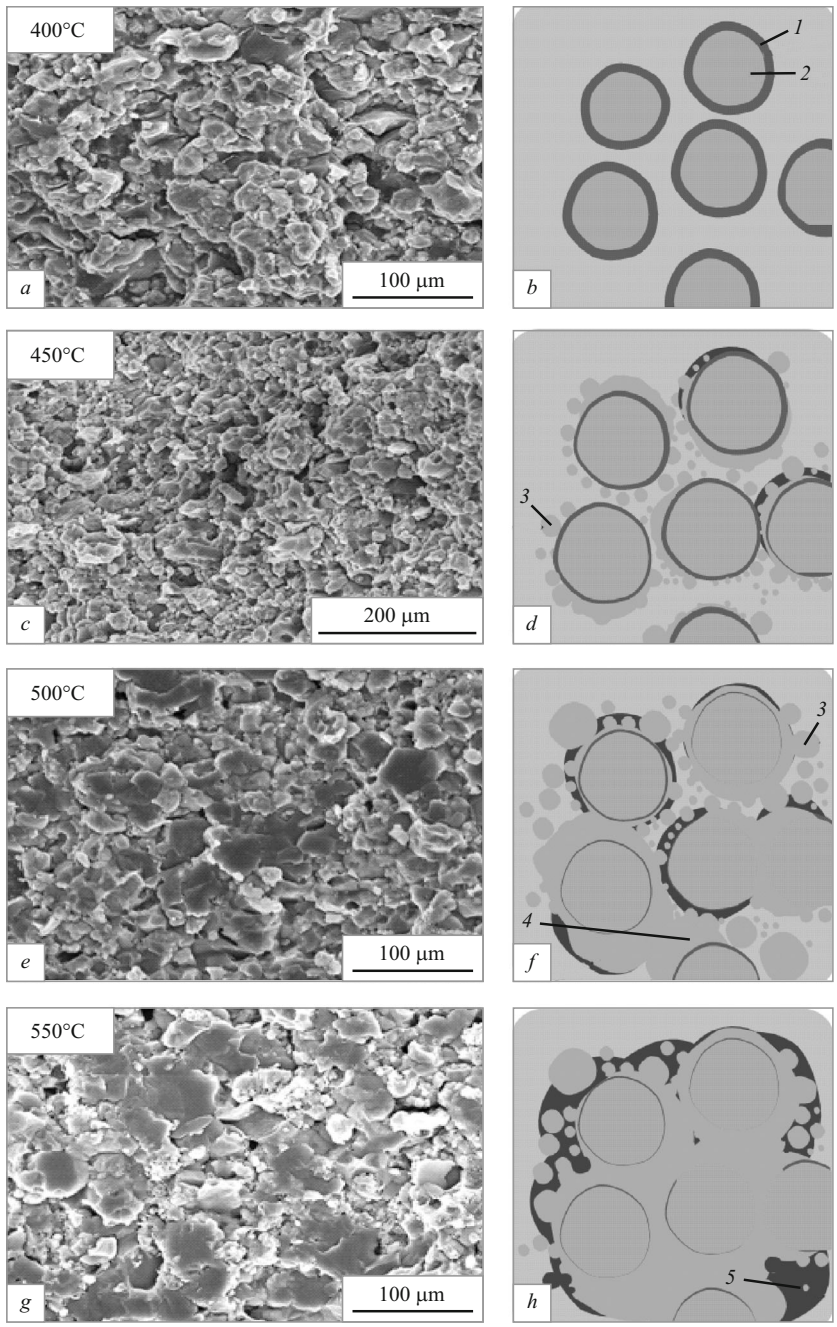

Fig. 5. Structure (SEM) of the cross section of Al – Cu core – shell particles sintered at different temperatures (*a*, *c*, *e*, *g*), and a schematic representation of their phase composition (*b*, *d*, *f*, *h*): *1*) copper shell; *2*) aluminium core; *3*) $CuAl_2$; *4*) interparticle bonds; *5*) CuAl.

3. An increase in the sintering temperature of particles reduces the electrical resistivity of the material due to the growth of crystalline grains and a decrease in porosity.

4. Addition of 3 – 6 wt.% glass frit to the powder effectively reduces the electrical resistivity of the material by increasing the bond between particles and reducing porosity. However, higher glass frit amount creates an insulating layer between the conductive particles, which leads to an increase in the electrical resistivity of the material.

5. A powder material sintered at 550°C from aluminium particles (core) with a copper coating (shell) with the addition of 3 wt.% glass frit has the highest conductivity. The electrical resistivity of this material is $1.01 \times 10^{-7}\ \Omega \cdot \text{m}$.

REFERENCES

1. G. Li, X. X. Huang, and J. K. Guo, "Fabrication and mechanical properties of Al_2O_3 – Ni composite from two different powder mixtures," *Mater. Sci. Eng. A*, **352**(1 – 2), 23 – 28 (2003).
2. T. Puclin and W. A. Kaczmarek, "Synthesis of alumina-nitride nanocomposites by successive reduction-nitridation in mechanochemically activated reactions," *J. Alloy. Compd*., **266**(1 – 2), 283 – 292 (1998).
3. G. M. Shi, J. K. Han, Z. D. Zhang, et al., "Pretreatment effect on the synthesis of Ag-coated Al_2O_3 powders by electroless deposition process," *Surf. Coat. Technol*., **195**(2 – 3), 333 – 337 (2005).

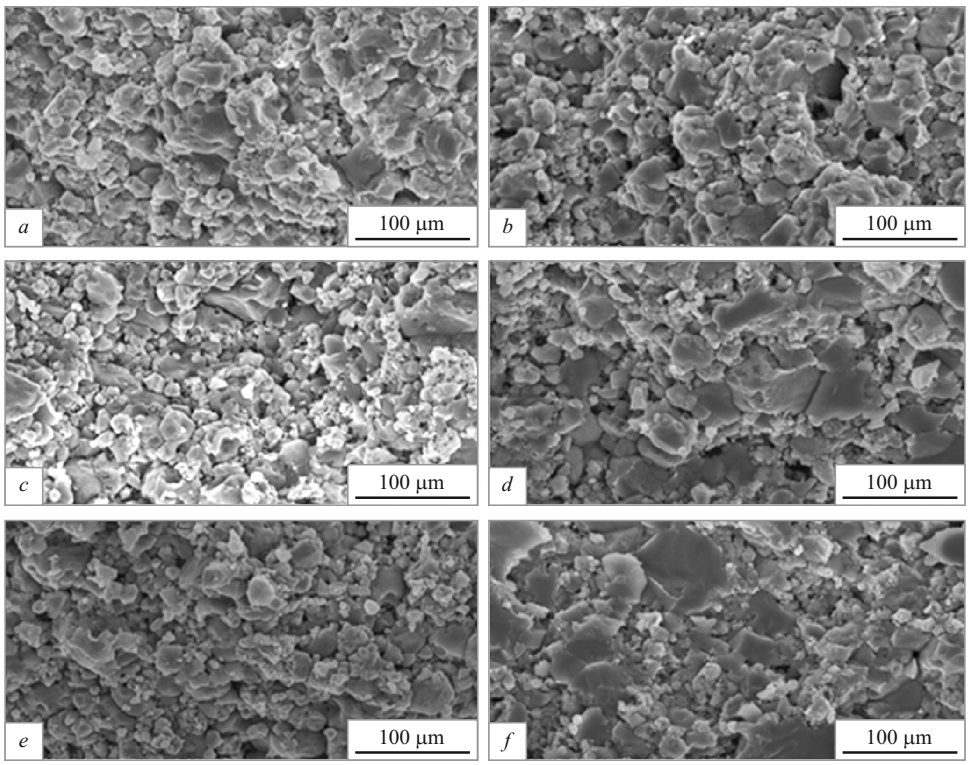

Fig. 6. Structure (SEM) of the cross section of Al – Cu core – shell particles sintered at 500°C (*a*, *c*, *e*) and 550°C (*b*, *d*, *f*), with a glass frit content: *a*, *b*) 3 wt.%; *c*, *d*) 6 wt.%; *e*, *f*) 9 wt.%.

4. V. V. Srdić, B. Mojić, M. Nikolić, and S. Ognjanović, "Recent progress on synthesis of ceramics core/shell nanostructures," *Process. Appl. Ceram*., **7**(2), 45 – 62 (2013).
5. T. Ji, V. G. Lirtsman, Y. Avny, and D. Davidov, "Preparation, characterization, and application of Au-shell/polystyrene beads and Au-shell/magnetic beads," Adv. Mater., **13**(16), 1253 – 1256 (2001).
6. J. Chen, B. Wiley, J. McLellan, et al., "Optical properties of Pd – Ag and Pt – Ag nanoboxes synthesized via galvanic replacement reactions," *Nano Lett*., **5**(10), 2058 – 2062 (2005).
7. W. Stöber, A. Fink, and E. Bohn, "Controlled growth of monodisperse silica spheres in the micron size range," *J. Colloid. Interf. Sci*., **26**(1), 62 – 69 (1968).
8. N. R. Jana, C. Earhart, and J. Y. Ying, "Synthesis of water-soluble and functionalized nanoparticles by silica coating," *Chem. Mater.*, **19**(21), 5074 – 5082 (2007).
9. D. V. Matyushov, "Standard electrode potential, Tafel equation, and the solvation thermodynamics," *J. Chem. Phys*., **130**(23), 234704 (2009).
10. K. C. Chuang and W. H. Lee, "Improvement on conductivity for thick film aluminum paste," *J. Nanosci. Nanotechnol*., **21**(9), 4726 – 4734 (2021).
11. J. Li, J. W. Mayer, and E. G. Colgan, "Oxidation and protection in copper and copper alloy thin films," *J. Appl. Phys*., **70**(5), 2820 – 2827 (1991).
12. C. Xu, Y. Liu, J. Wang, et al., "Fabrication of nanoporous Cu – Pt(Pd) core/shell structure by galvanic replacement and its application in electrocatalysis," *ACS Appl. Mater. Interf*., **3**(12), 4626 – 4632 (2011).
13. T. Gustmann, J. M. dos Santos, P. Gargarella, et al., "Properties of Cu-based shape-memory alloys prepared by selective laser melting," *Shap. Mem. Superelasticity*, **3**(1), 24 – 36 (2017).
14. S. Zeller and J. Gnauk, "Shape memory behavior of Cu – Al wires produced by horizontal in-rotating-liquid-spinning," *Mater. Sci. Eng. A*, **481**, 562 – 566 (2008).
15. S. Yu. Kondrat'ev and O. V. Shvetsov, "Effect of high-temperature heating on the structure and properties of aluminum alloys in the production of drill pipes," *Met. Sci. Heat Treat*., **55**(3 – 4), 191 – 196 (2013).
16. A. T. Adorno and R. A. G. Silva, "Ageing behavior in the Cu – 10 wt.% Al and Cu – 10 wt.% Al – 4 wt.% Ag alloys," *J. Alloy. Compd*., **473**(1 – 2), 139 – 144 (2009).